

Large angle radiation effect on jet measurement in pp collisions at $\sqrt{s}=7$ TeV at the LHC*

Ren-Zhuo Wan(万仁卓)^{1;1)} Si-Yuan Wang(王思源)¹ Shuang Li(李双)³ Yi-Ming Feng(冯绎铭)¹
Feng Liu(刘丰)¹ Fan Yang(杨帆)¹ Dai-Cui Zhou(周代翠)^{2;2)}

¹ Nano-Optical Material and Storage Device Research Center, School of Electronic and Electrical Engineering, Wuhan Textile University, Wuhan 430200, China

² Key Laboratory of Quark and Lepton Physics (MOE) and Institute of Particle Physics, Central China Normal University, Wuhan 430079, China

³ College of Science, China Three Gorges University, Yichang 443002, China

Abstract: Jet measurement is an ideal probe to explore the properties of the hot dense matter created in ultra-relativistic heavy-ion collisions. Recent results at the LHC show that large angle radiation is non-negligible, but the mechanisms and phenomenology of large angle radiation are still unclear and hotly debated. Considering the coexistence and competition of different physics mechanisms qualitatively, it is assumed that the radiation angle is enhanced randomly over a wide range based on the collinear approximation. Its effects on di-jet momentum imbalance, jet fragmentation function and jet shape are studied in pp collisions at 7 TeV. The results show that di-jet asymmetry is insensitive to large angle radiation, while jet shape and jet fragmentation functions are more sensitive and could explain experimental data well. We conclude that de-collimated radiation cannot be ignored for soft jets, and there is a contribution from large angle radiation ($\phi > 0.7$) of about 8%, which is significant for jet intrinsic structure measurement at $p_{T,\text{jet}} < 80$ GeV/c.

Keywords: quark gluon plasma, jet quenching, di-jet, large angle radiation, jet shape

PACS: 52.20.Hv, 52.20.Fs, 29.30.Dn **DOI:** 10.1088/1674-1137/42/11/114001

1 Introduction

The Large Hadron Collider (LHC) has opened a new era to explore the properties of hot dense QCD matter, quark-gluon plasma (QGP). Jets which are produced by partons at an early stage from the colliding nuclei will travel through QCD matter and carry full evolution information, and are thus an ideal probe. One of the most striking discoveries is jet quenching [1–5], by the measurement of hadron or jet spectra prolonged from pp to pA or AA collisions, which provides an overall suppression effect. Detailed measurements of jet characteristics arising from the complicated jet-medium interaction are crucial to explore the micro-jet modification formalism within the pQCD framework.

Recent measurements of di-jet asymmetry [6, 7] have found more highly unbalanced di-jets with increasing event centrality. Inclusive jet suppression of about a factor of two is observed in central heavy-ion collisions, relative to peripheral collisions. There is also a weak

dependence on jet radius and transverse momentum [8]. A reduction of fragment yield at intermediate z and enhancement at small z have also been found in central collisions relative to peripheral collisions [9, 10]. The excess yield in azimuthal di-hadron correlations is found to be more pronounced on the sub-leading jet side at low p_T [11]. In addition, charged particle nuclear modification factor measurements [12] show a sectionalized behavior, with a local maximum at $p_T \approx 2$ GeV, decreasing to a minimum at $p_T \approx 7$ GeV, then going up to $p_T \approx 60$ GeV and then becoming less steep. A more important discovery is that partons redistribute and lose energy for sub-leading jets predominantly from several to 20 GeV, arising from soft particles being radiated at large angles with respect to the direction of the original parton. Those results indicate complicated parton-medium interactions in the soft region and non-pQCD hard region.

Most phenomenological studies of jet evolution and energy loss, such as the quenching weight method [13], modified DGLAP evolution equation [14], HT [15], GLV

Received 5 June 2018, Published online 13 October 2018

* Supported by National Natural Science Foundation of China (11505130, 11775097, IRG1152106, 11475068) and CTGU (1910103, B2018023)

1) E-mail: wanrz@wtu.edu.cn

2) E-mail: dczhou@mail.cnu.edu.cn

©2018 Chinese Physical Society and the Institute of High Energy Physics of the Chinese Academy of Sciences and the Institute of Modern Physics of the Chinese Academy of Sciences and IOP Publishing Ltd

[16], AMY [17], etc., describe the data well in the intermediate momentum range, but are insufficient to cover the full kinematic range. The crucial reason is the treatment of gluon radiation and momentum exchange in the medium, by supposing collinear radiation gives rise to a small angle radiation. In this paper, considering the coexistence and competition of physics mechanisms, it is assumed that the radiation angles are enhanced randomly based on a collinear formalism in a qualitative way in pp collisions, as a baseline for further work on heavy-ion collisions. The large angle radiation effect on jet measurement of di-jet momentum asymmetry, jet fragmentation function, and jet shape is studied in detail using JEWEL [18].

2 Large angle radiation

In the jet evolution picture, hard partons carry most of the jet energy and, without suffering medium interaction, can be considered as surface emission. Soft partons experience stronger medium modification by medium-induced gluon radiation, based on approximations such as the eikonal, soft or collinear approximations, thus giving rise to small angle radiation with typical transverse momentum, ~ 1 GeV. For a process $a \rightarrow bc$, the branching angle is usually given as in Eq. (1):

$$\theta_a \approx \frac{p_{T,b}}{E_b} + \frac{p_{T,c}}{E_c} = \frac{1}{\sqrt{z_a(1-z_a)}} \frac{m_a}{E_a}. \quad (1)$$

Actually, when partons traverse the medium, various effects such as recoil and non-recoil, coherence and de-coherence, coexist and compete depending on the medium density, path length, gluon formation time and momentum exchange etc. This may break the collinear or eikonal limit in model prediction. Besides, the boundary definitions between collinear and de-collinear radiation, coherence and de-coherence, as well as the eikonal and non-eikonal limit, are strongly model-dependent. Large angle radiation should exist over a wide momentum range directly or by multiple interactions. Different methods have been studied, such as the fifth form factor [19], momentum kick model [20], AMPT model [21], inelastic interaction beyond eikonal approximation [22] and elastic contribution [23], jet-induced flow [24], and wave turbulence [25], indicating the non-ignorable phenomena for the parton-medium interaction.

To further understand the mechanism from new LHC data, this paper is based on the fact that hard gluon emission has a low production rate and is beyond the pQCD capability, and semi-soft gluon emission is largely erased by clustering process into jets, while the dynamics of soft gluons are generic and independent of specific model assumptions. It is reasonable to relax the previous approximations in a qualitative way and build large angle radiation phenomena. In this paper, the radiation

angles based on Eq. (1) are enhanced randomly, so as to estimate jet shower topology modifications by the observations of jet fragmentation function, jet shape and di-jet momentum asymmetry.

3 Simulation method

In this study, JEWEL is used to simulate jet production, QCD scale evolution and re-scattering of jets in heavy-ion collisions based on pQCD. It describes the jet evolution and jet-medium interactions simultaneously and dynamically based on leading-order matrix elements plus parton shower method. Soft gluon radiation, recoil effect and scattering processes are governed by formation time. The LPM effect is included by generalizing the probabilistic formulation in the eikonal limit to general kinematics. The initial temperature is set to $T_i=0.4$ GeV for proton-proton collisions at 7 TeV. Jets are reconstructed with the anti-kt algorithm provided by the Fast-Jet package, with a radius parameter of $R=0.6$ within $|\eta| < 2.8$.

The di-jet events are produced in proton-proton collisions at a center of mass of 7 TeV. The opening angle of the radiated gluon is randomly magnified by 20% and 40% (referred to as Angle_v1 and Angle_v2 respectively) with respect to Eq. (1) (referred to as Angle_v0). The obtained wide opening angle distribution from simulation is shown in Fig. 1. About 40% of the partons are radiated at a smaller angle ($\phi < 0.1$). The intermediate angles ($0.1 < \phi < 0.7$) are shifted to larger angles which are a little bit lower than Angle_v0. About 8% of the partons are radiated at larger angles ($\phi > 0.7$) which are higher than Angle_v0.

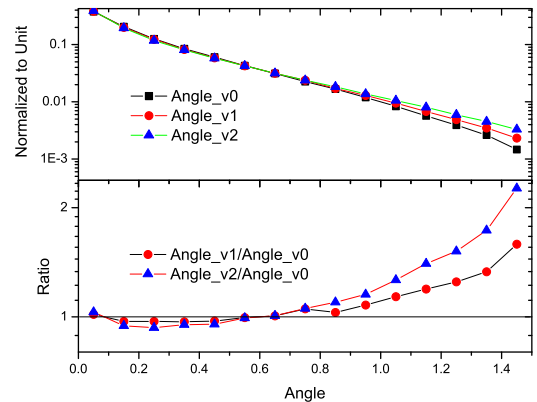


Fig. 1. (color online) Branching angle (for $a \rightarrow bc$) distributions under three configurations (top) and their ratios (bottom).

4 Results and discussion

The di-jet energy asymmetry is defined as Eq. (2), which is obtained from all final jet energy fluctuations at

hadronic level regardless of their origin.

$$A_J = \frac{|p_{T,1} - p_{T,2}|}{p_{T,1} + p_{T,2}} \quad (2)$$

One of most striking features of the di-jet momentum imbalances in Refs. [6, 7] are that significant jet energy is dissipated to large angles. Most of the models can match the data well at jet hadronic level and are strongly dependent on jet selection. However, there is still no clear and quantitative explanation. It was found in Ref. [26] that di-jet asymmetry is not sensitive to model and hydrodynamical evolution. In Refs. [27, 28], the results indicate that A_J is sensitive to the jet-medium interaction mechanism and insensitive to hadronization and final state hadron re-scattering. However, in Ref. [29] the authors found that A_J is most sensitive to \hat{q} and relatively insensitive to the nature of the jet-medium interaction mechanism. Those studies are directly related to the formulism of gluon radiation or parton scattering, and especially to the branching angles.

The di-jet asymmetry and azimuthal angle between the two jet $\Delta\phi$ distributions from JEWEL and data are shown in Fig. 2. We use the same jet selection criteria

as in Ref. [6], where the leading jet $p_{T,1} > 100$ GeV/c and opposite sub-leading jet $p_{T,2} > 25$ GeV/c are required, and di-jet azimuthal angles $\Delta\phi > \pi/2$. It can be seen from Fig. 2(a) and (b) that with increasing jet p_T , the di-jets are better balanced in energy asymmetry at $A_J = 0$ and in back-to-back azimuthal angles at $\Delta\phi = \pi$, and are close to stable when $p_T > 100$ GeV/c. The data can be considered as a superposition from different $p_{T,\text{jet}}$ bins, which is directly related to di-jet production cross section. This may explain why most of the models can explain the data well. Besides, Fig. (2)(c) and (d) clearly show the di-jet asymmetry evolution from the initial two hard partons, to parton shower jets, and reconstructed di-jets under three radiation angle configurations. The large angle radiation effect can be ignored when $A_J < 0.3$ and there is very little difference at larger momentum imbalance. The two jet $\Delta\phi$ distribution indicates a weak modification by large angle radiation. This is consistent with the large angle radiation assumption, since the partons radiated from small and intermediate angles could be incorporated into the jet and only a small fraction of energy escape for a hard jet at $p_{T,\text{jet}} > 80$ GeV/c.

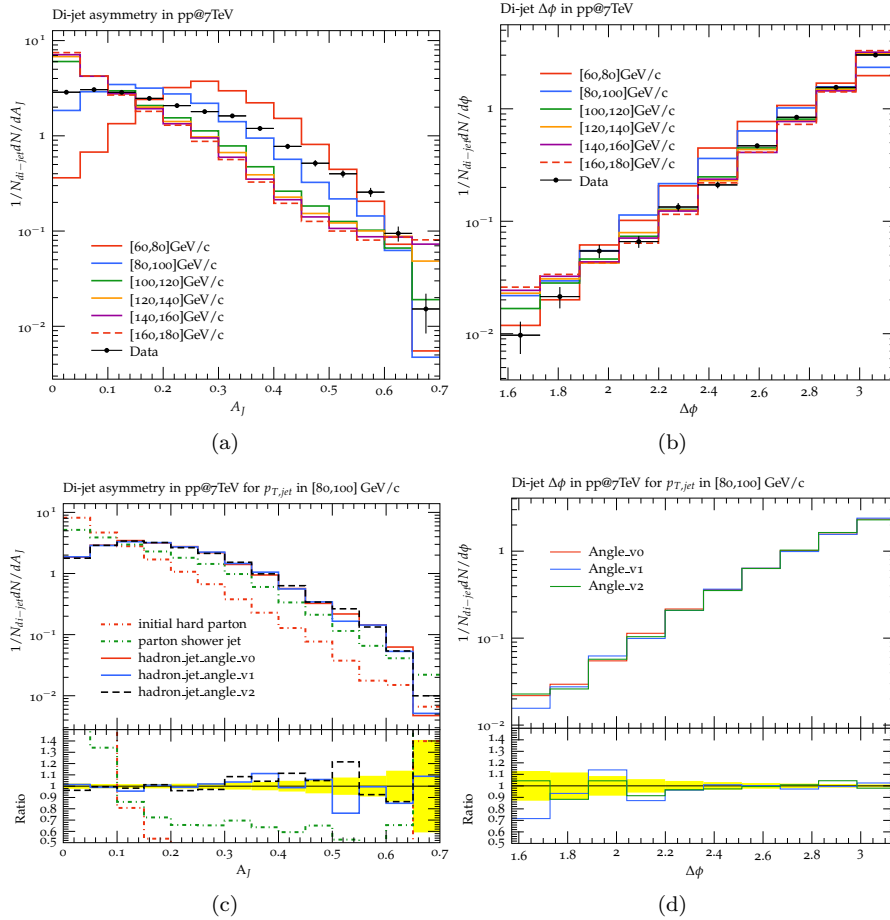


Fig. 2. (color online) Di-jet asymmetry (a and c) and azimuthal angle between the two jet $\Delta\phi$ (b and d) distributions from JEWEL+PYTHIA (lines) compared with data from pp collisions at 7 TeV (black points) [6]. (c) and (d) are plotted for $80 \text{ GeV}/c < p_{T,\text{jet}} < 100 \text{ GeV}/c$.

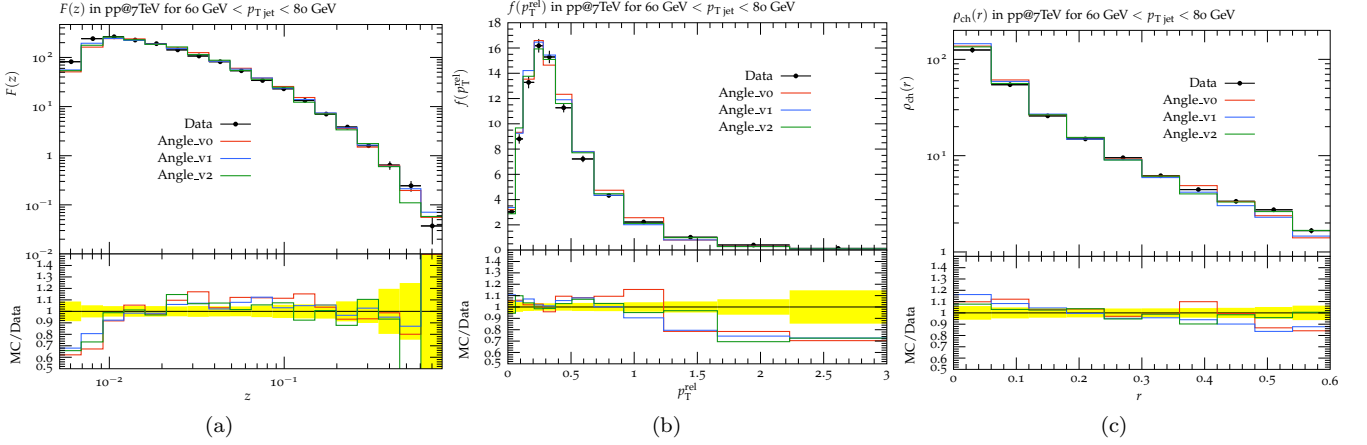


Fig. 3. (color online) Distribution of $F(z)$, $f(p_T^{\text{jet}})$ and $\rho(r)$ for $60 \text{ GeV}/c < p_{T,\text{jet}} < 80 \text{ GeV}/c$ under the three radiation angle configurations by JEWEL+PYTHIA compared with data (black points) [30].

It is important to relate jet fragmentation to the complex parton fragmentation process, and its intrinsic structure is sensitive to the gluon radiation pattern. The fragmentation function $D_i^h(z, Q)$ is defined as the probability that a hadron carries a longitudinal momentum fraction z of the parton (jet), where z and $F(z, p_{T,\text{jet}})$ are defined as Eq. (3) and Eq. (4) respectively:

$$z = \frac{\vec{p}_{\text{jet}} \cdot \vec{p}_{\text{ch}}}{|\vec{p}_{\text{jet}}|^2}, \quad (3)$$

$$F(z, p_{T,\text{jet}}) = \frac{1}{N_{\text{jet}}} \frac{dN_{\text{ch}}}{dz}, \quad (4)$$

where \vec{p}_{jet} is the momentum of the reconstructed jet and \vec{p}_{ch} is the momentum of the charged particles. N_{ch} is the number of charged particles in the jet. p_T^{rel} is the momentum of charged particles in a jet transverse to the jet's axis, defined as in Eq. (5), and its distribution $f(p_T^{\text{rel}}, p_{T,\text{jet}})$ is defined as in Eq. (6):

$$p_T^{\text{rel}} = \frac{|\vec{p}_{\text{ch}} \times \vec{p}_{\text{jet}}|}{|\vec{p}_{\text{jet}}|}, \quad (5)$$

$$f(p_T^{\text{rel}}, p_{T,\text{jet}}) = \frac{1}{N_{\text{jet}}} \frac{dN_{\text{ch}}}{dp_T^{\text{rel}}}. \quad (6)$$

The density of charged particle ρ_{ch} in $y-\phi$ space is measured as a function of angular distance r of charged particles from the jet axis, given by:

$$\rho_{\text{ch}} = \frac{1}{N_{\text{jet}}} \frac{dN_{\text{ch}}}{2\pi r dr}. \quad (7)$$

The distributions of $F(z)$, $f(p_T^{\text{jet}})$ and $\rho(r)$ are simulated for $5 \text{ GeV}/c < p_{T,\text{jet}} < 300 \text{ GeV}/c$. The results show that three distributions are in reasonable agreement with data for the three radiation angle configurations at $p_{T,\text{jet}} > 80 \text{ GeV}/c$. However, for $p_{T,\text{jet}} < 80 \text{ GeV}/c$, there are slight differences from data, as shown in Fig. 3 for $60 \text{ GeV}/c < p_{T,\text{jet}} < 80 \text{ GeV}/c$ under the three radiation angle configurations compared with data

(black points). At intermediate z , $F(z)$ can match the data well, but it shows about 30% deviation at lower z . The distributions $f(p_T^{\text{jet}})$ and $\rho(r)$ describe the shape of jets transverse to the jet direction well for $p_T^{\text{rel}} < 1 \text{ GeV}/c$ and independent of r . From the overall view at $p_{T,\text{jet}} < 80 \text{ GeV}/c$, with larger radiation angle configurations, the simulations are closer to data. Due to the nature of fragmentation measurement in experiments, which is strongly dependent on jet reconstruction, the fragmentation is insensitive to larger angle radiation.

In addition, jet shape related observables can better quantify the jet internal structure and tomography, which is directly connected to the soft contributions of multiple gluon emission and medium interaction, as well as non-perturbative fragmentation. The jet internal structure is studied in terms of differential and integrated jet shapes from reconstructed jets. Differential jet shape $\rho(r)$ is defined as the average fraction of the jet transverse momentum that lies inside an annulus of inner radius $r - \Delta r/2$ and outer radius $r + \Delta r/2$ around the jet axis, as defined in Eq. (8):

$$\rho(r) = \frac{1}{\Delta r} \frac{1}{N_{\text{jets}}} \sum_{\text{jets}} \frac{p_T(r - \Delta r/2, r + \Delta r/2)}{p_T(0, R)}, \quad (8)$$

where $\Delta r \leq r \leq R - \Delta r/2$, $p_T(r_1, r_2)$ denotes the sum of clusters in the annulus between r_1 , and r_2 , N_{jet} is the number of jets. $\sum_0^R \rho(r) \Delta r = 1$ by definition. Alternatively, the integrated jet shape $\psi(r)$ is defined as the average fraction of the jet p_T that lies inside a cone radius r concentric with the jet cone:

$$\psi(r) = \frac{1}{N_{\text{jets}}} \sum_{\text{jets}} \frac{p_T(0, r)}{p_T(0, R)}. \quad (9)$$

The results show that the simulations describe the data well at $p_{T,\text{jet}} > 60 \text{ GeV}/c$. However, at $p_{T,\text{jet}} < 60 \text{ GeV}/c$ the simulations do not match the data well. Here, the differential jet shape and integrated jet shape $\rho(r)$ for

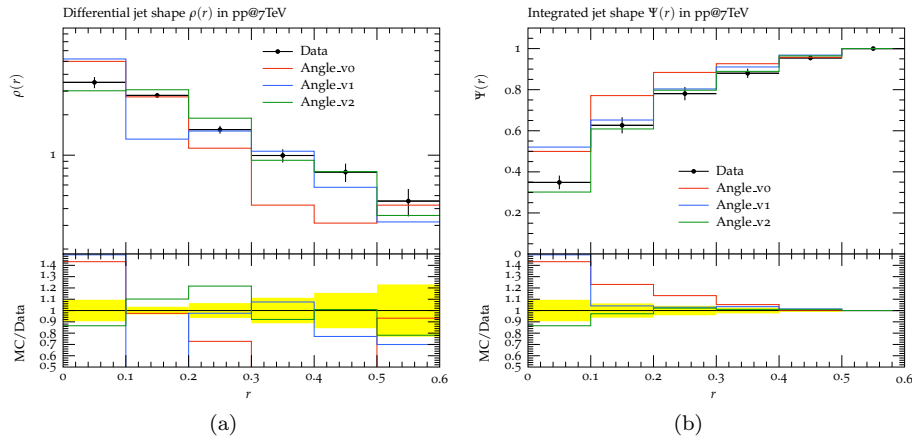


Fig. 4. (color online) The differential jet shape $\rho(r)$ and differential jet shape $\psi(r)$ for $30 \text{ GeV}/c < p_{T,\text{jet}} < 40 \text{ GeV}/c$ and $|\eta| < 2.8$ at the three radiation angle configurations from JEWEL+PYTHIA, compared with data [31] from pp collisions at 7 TeV.

$30 \text{ GeV}/c < p_{T,\text{jet}} < 40 \text{ GeV}/c$ and $|\eta| < 2.8$ are shown in Fig. 4. It can be seen that the jet shape observables better match the data at larger angle configurations, which is also consistent with Fig. 3(c). In the absence of a medium recoil effect, the gluon radiation angle is related to the distance r . For $p_{T,\text{jet}} > 60 \text{ GeV}/c$, parton fragmentation is harder and more collimated than in softer jets. The probability of non-perturbative fragmentation should be larger for soft jets.

5 Conclusion

Based on the assumption of different coexisting and competing physics mechanisms, larger angle radiation is imposed randomly for partons going through QCD mat-

ter. It is simulated by JEWEL for proton-proton collisions at 7 TeV. Di-jet asymmetry, jet fragmentation function and jet shape are analyzed and compared with data. The results show that di-jet asymmetry, as a macro measurement of the jets, is less sensitive to gluon radiation angles. The differences for jet fragmentation and jet shape are clear for $p_{T,\text{jet}} < 80 \text{ GeV}/c$, and simulation results describe the data well for larger angle radiation configurations. We conclude that hard jet fragmentation is harder and more collimated than softer jets and there is a contribution of about 8% from large angle radiation ($\phi > 0.7$) in pp collisions at 7 TeV, which is non-negligible for soft jet intrinsic structure measurement and should be investigated further.

References

- 1 K. Adcox et al (PHENIX Collaboration), Phys. Rev. Lett., **88**: 022301 (2002)
- 2 C. Adler et al (STAR Collaboration), Phys. Rev. Lett., **89**: 202301 (2002)
- 3 K. Aamodt et al (ALICE collaboration), Phys. Lett. B, **696**: 30-39 (2011)
- 4 G. Aad et al (ATLAS Collaboration), Phys. Rev. Lett., **114**: 072302 (2015)
- 5 K. Aamodt et al (ALICE collaboration), Phys. Lett. B, **746**: 1-14 (2015)
- 6 G. Aad et al (ATLAS collaboration), Phys. Rev. Lett., **105**: 252303 (2010)
- 7 V. Khachatryan et al (CMS collaboration), Phys. Rev. C **84** : 024906 (2011)
- 8 G. Aad et al (ATLAS collaboration), Phys. Lett. B, **719**: 220-241 (2013)
- 9 G. Aad et al (ATLAS collaboration), Phys. Lett. B, **739**: 320-342 (2014)
- 10 G. Aad et al (ATLAS collaboration), Eur. Phys. J. C, **77**(6): 379 (2017)
- 11 V. Khachatryan et al (CMS collaboration), JHEP, **11**: 055 (2016)
- 12 G. Aad et al (ATLAS collaboration), JHEP, **09**: 050 (2015)
- 13 Carlos A. Salgado, Urs Achim Wiedemann, Phys. Rev. D, **68**: 014008 (2013)
- 14 Ning-Bo Chang, Wei-Tian Deng, and Xin-Nian Wang, Phys. Rev. C, **89**: 034911 (2014)
- 15 X. f. Guo and X. N. Wang, Phys. Rev. Lett., **85**: 359 (2000)
- 16 M. Gyulassy, P. Levai and I. Vitev, Phys. Lett. B, **594**: 371 (2001)
- 17 P. B. Arnold, G. D. Moore, and L. G. Yaffe, JHEP, **030**: 0206 (2002)
- 18 Korinna C. Zapp, Eur. Phys. J. C, **74**: 2762 (2014)
- 19 Yu.L. Dokshitzer, G. Marchesini, JHEP, **01**: 007 (2006)
- 20 Cheuk-Yin Wong, Phys. Rev. C, **84**: 024901 (2011)
- 21 Zhan Gao, Ao Luo, Guo-Liang Ma, Guang-You Qin, and Han-Zhong Zhang, Phys. Rev. C, **97**: 044903 (2018)
- 22 Raktim Abir, Phys. Rev. D, **87**: 034036 (2013)
- 23 Guang-You Qin, Berndt Müller, Phys. Rev. Lett., **106**: 162302 (2011)
- 24 Yasuki Tachibana, Ning-Bo Chang, and Guang-You Qin, Phys. Rev. C, **95**: 044909 (2017)
- 25 Edmond Iancu, Nucl. Phys. A, 932 : 197-204 (2014)
- 26 Thorsten Renk, Phys. Rev. C, **85**: 064908 (2012)
- 27 Guo-Liang Ma, Phys. Rev. C, **87**: 064901 (2013)
- 28 Florian Senzel, Oliver Fochler, Jan Uphoff, Zhe Xu, and Carsten Greiner, J. Phys. G, **42**(11): 115104 (2015)
- 29 Christopher E Coleman-Smith, Berndt Müller, Phys. Rev. C, **86**: 054901 (2012)
- 30 G. Aad et al (ATLAS collaboration), Eur. Phys. J. C, **71**:1795 (2011)
- 31 G. Aad et al (ATLAS collaboration), Phys. Rev. D, **83**: 052003 (2011)